LAWRENCE
LIVERMORE
NATIONAL
LABORATORY

UCRL-CONF-232164

Investigating the Stability and Accuracy of the Phase Response for NOx Sensing 5% Mg-modified LaCrO3 Electrodes

E. P. Murray, R. F. Novak, D. J. Kubinski, R. E. Soltis, J. H. Visser, L. Y. Woo, L. P. Martin, R. S. Glass

June 26, 2007

The 211th Electrochemical Society Meeting
Chicago, IL, United States
May 6, 2007 through May 10, 2007

Updated October 14, 2003

UCRL-CONF-232164

Investigating the Stability and Accuracy of the Phase Response for NO_x Sensing 5% Mg-modified $LaCrO_3$ Electrodes

E. Perry Murray, R.F. Novak, D.J. Kubinski, R.E. Soltis, J.H. Visser, L. Woo, L.P. Martin and R. Glass

Abstract

Impedance spectroscopy measurements were carried out on $LaCr_{0.95}Mg_{0.05}O_3$ (LCM) asymmetric interdigitated electrodes supported on fully stabilized 8-mol% Y_2O_3-stabilized ZrO_2 (YSZ) electrolytes. Experiments were carried out using 0 – 50 ppm NO_x, 5 – 15% O_2 with N_2 as the balance, over temperatures ranging from 600 – 700°C. AC measurements taken at a constant frequency between 1 – 100 Hz indicated the phase response of the sensor was less sensitive to fluctuations in the O_2 concentration and the baseline drift was limited. Specific frequencies were observed where the sensor response was essentially temperature independent.

Introduction

NO_x exhaust gas sensors are a critical component for the control strategies intended for MY2010 diesel after treatment systems. Current NO_x sensors are capable of accurately measuring NO_x at levels down to about 10 ppm. However, as emissions standards tighten it will become necessary to detect substantially lower NO_x emissions. For example, to achieve the MY2010 Tier 2 Bin 5 OBD emissions standards for light duty diesel vehicles a suitable NO_x sensor may need to detect NO_x at levels as low as 1 – 2 ppm.[1] Such requirements drive the need for far more accurate NO_x sensors that are capable of demonstrating greater stability, sensitivity and selectivity.

Metal oxide electrodes have received a great amount of attention in recent years as the NO_x sensing performance of these electrodes can be substantially greater than that observed from standard Pt electrodes. Numerous spinel and perovskite type oxides have been screened in studies focusing on NO_x sensitivity and selectivity, and the results are summarized in review articles.[2,3] Fewer studies have investigated the accuracy of such sensing electrodes which strongly depends upon the electrode response time and stability. In one study using lean-burn gasoline engines, it was reported that sensors with Cr_2O_3 electrodes were capable of detecting NO_x with errors no larger than 10% for NO_x levels ranging from 45 – 306 ppm.[4] However, other studies found the oxygen response time of Cr_2O_3 electrodes was too slow to be practical.[5] In addition to having a rapid response time, the electrode must be chemically and electrically stable. Studies show that b-site doping in perovskites resulted in greater chemical stability in comparison to a-site doping.[6] Preliminary experiments by the authors on $LaCrO_3$ electrodes doped with Sr on the a-site and Mg on the b-site found the a-site doped electrodes decomposed under certain conditions; whereas, the b-site doped electrodes remained stable under a range of operating conditions in the various exhaust gas atmospheres.

Presented in this paper are the NO_x sensing characteristics for 5% Mg-modified $LaCrO_3$ (LCM) electrodes that were measured using AC impedance techniques. The real, imaginary and phase components of the impedance were investigated in order to interpret the NO_x sensing behavior of LCM electrodes under AC conditions. The stability of this sensor with respect to fluctuations in operating temperature and oxygen concentration is also discussed.

Experimental

Figure 1 shows an image of the sensor with LCM asymmetric interdigitated electrodes (IDE). The fully stabilized 8-mol% Y_2O_3-stabilized ZrO_2 support was tape cast and fired at 1400°C for 2 hours. The LCM electrodes were screen printed over the substrate and sintered at 1200°C for 1 hour. To insure sufficient current collection a Ag-Pd overlay was applied and fired at 900°C for 1 hour. Further details concerning the fabrication procedure are described elsewhere.[7] The fired sensor was 17 mm in diameter and approximately 2 mm thick. The thick and thin IDE had a thickness of 30 μm. Au wires were attached from the outer edges of the IDE using Au paste and a ZrO_2-based cement.

Figure 1

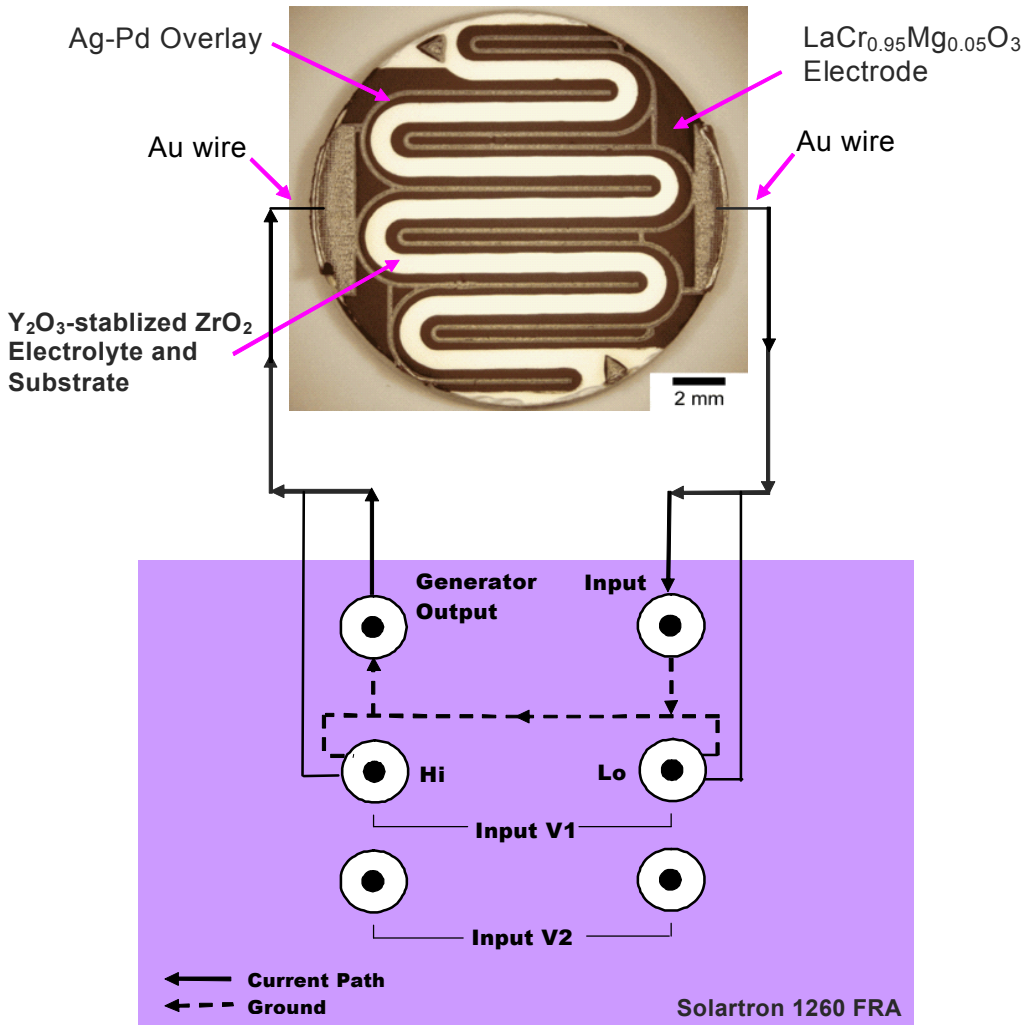

Figure 1. Photograph of LCM/YSZ sensor prior to testing, along with illustration of wiring connections made to the 1260 Solartron Impedance Analyzer.

Impedance spectroscopy measurements were carried out using a 1260 Solartron FRA (frequency response analyzer). The frequency range studied was from 0.1 Hz to 10^7 Hz. The applied signal amplitudes were 10, 50, 75 and 100 mV; although, most experiments were carried out using a 50 mV signal. Measurements were performed at open circuit for temperatures ranging from 600 – 700°C in NO_x atmospheres of 0 – 50 ppm with 5 – 15% O_2 present. A gas

50:50 mixture of NO+NO_2 was used to determine any interference effects between NO and NO_2. Leads from the impedance analyzer were connected to the Au wires from the sensor as shown in Figure 1. Scanning electron micrograph (SEM) images were collected before and after completing the sensor measurements in order to verify the structure and detect any microstructural changes that may have occurred during operation.

Results and Discussion

Structure and Morphology

The SEM images shown in figure 2 illustrate the structure of the electrode prior to testing. The broad (~100 μm width) Ag-Pd overlay was considerably porous, even at the mid-point region shown in figure 2b. The porosity of the overlay was beneficial for sensor operation as it allowed gas diffusion; thereby, avoiding the formation of reaction "dead zones" that are commonly associated with overlays. Figure 2c shows the clear interface between the Ag-Pd overlay and LCM electrode, as well as a comparison between the two porous structures. At greater magnification it was evident that particles composing the electrode exhibited a high degree of particle-to-particle contact with limited necking (i.e., small contact area). Such a structure creates a high density of reaction sites that can promote sensor performance. Additionally, increasing the contact area between particles would improve the robustness of the electrode further aiding performance. The $ZrCr_2O_4$ crystals also noted in figure 2d resulted from the flux in the Ag-Pd overlay paste. Since $ZnCr_2O_4$ is known to detect NO_x[8], these crystals most likely contributed to the NO_x sensing performance of the electrode.

Figure 2

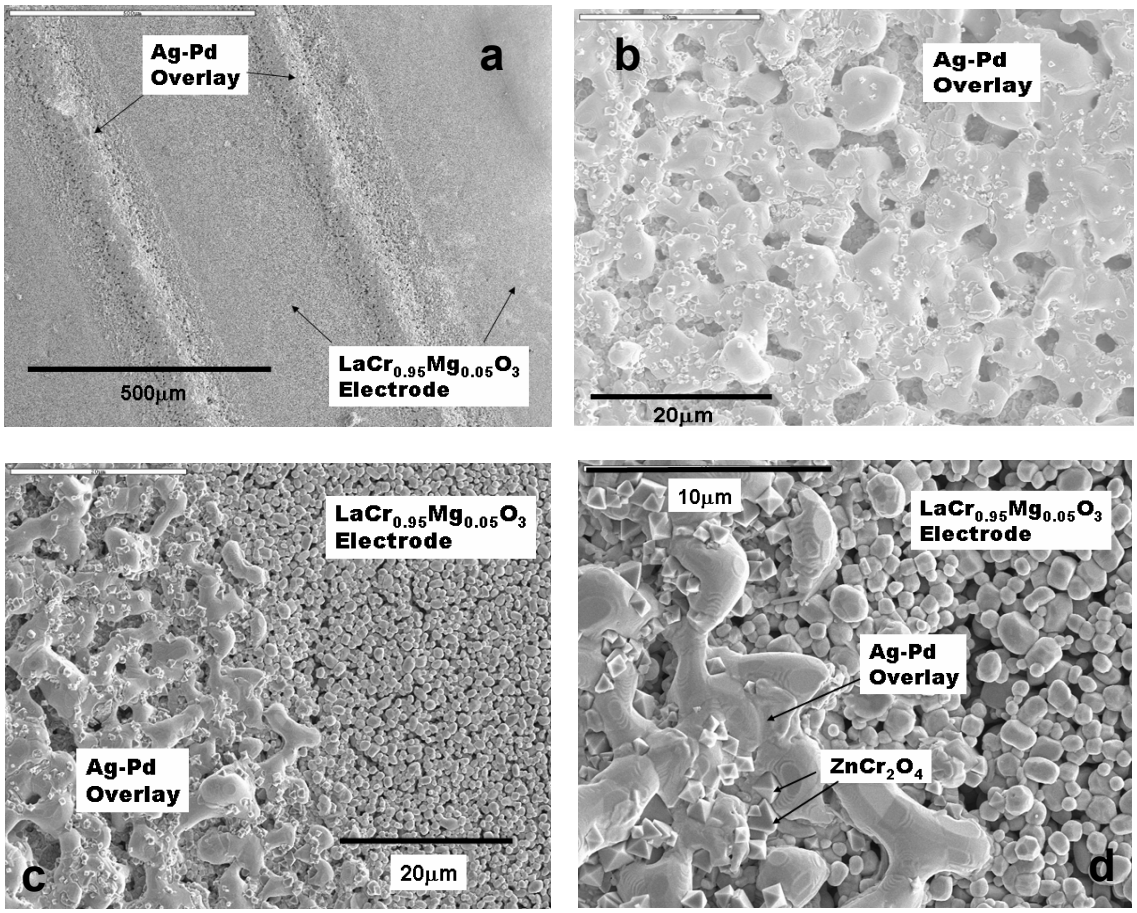

Figure 2. SEM images prior to testing of a) an LCM electrode with Ag-Pd overlay, b) the center region of the Ag-Pd overlay indicating substantial porosity, c) the interface between the overlay and electrode, and d) evidence of $ZnCr_2O_4$ crystals that were a byproduct of the Ag-Pd overlay flux.

NO_x and O_2 Sensitivity

The LCM sensor response in terms of the real, imaginary, and phase components of the impedance is shown in figure 3 for measurements collected at a constant frequency of 20 Hz for multiple signal amplitudes. A series of 50 ppm NO_x pulses were introduced into the gas stream while 5% or 10% O_2 was present in order to observe the NO_x and O_2 sensitivity of each of the 3 impedance components. The sensor response described by the real impedance in figure 3a does not depict any distinguishable features corresponding to the series of pulses for NO, NO_2 and the 50:50 NO+NO_2 mixture. Additionally, the real impedance response of the sensor shows

significant drift. The real impedance describes the resistance of the electrode. Since the real impedance was not sensitive to NO_x this indicates that NO_x does not change the LCM electrode resistance. On the other hand, the imaginary impedance data clearly reflects the gas cycling of the NO_x as shown in figure 3b. Again drift is evident, and the absolute value of the imaginary response drifted in the same direction as the real impedance response. The capacitive behavior of the electrode is described by the imaginary part. Thus, it is apparent from this data that the presence of NO_x significantly changed the capacitance of the LCM sensing electrode. The most intriguing data is shown in figure 3c where the phase of the impedance is plotted. The response to NO_x was much stronger and signal drift was quite limited. Equation 1 mathematically describes the phase as:

$$\theta = \arctan(Z''/Z') \qquad (1)$$

where Z' and Z'' are the real and imaginary parts of the impedance, respectively. Apparently, certain factors associated with drift are cancelled out or decrease in magnitude through this mathematical relationship. This behavior is not currently understood. However, in other studies the authors observed similar behavior at $(La,Sr)CrO_3$ sensing electrodes.

Figure 3 also illustrates the O_2 sensitivity of the various impedance components. By comparing the 5% and 10% O_2 data collected at a signal amplitude of 75 mV it is apparent that increasing the O_2 concentration lowers the absolute value of the real, imaginary and phase response. Though the O_2 affects the real and imaginary parts (i.e., the resistance and capacitance

Figure 3

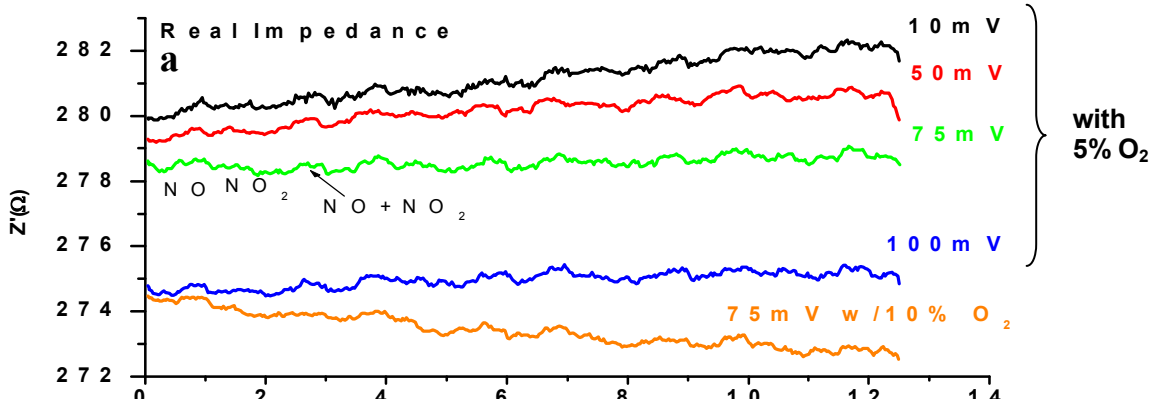

Figure 3. NO_x sensing response of the a) real, b) imaginary, and c) phase components of the impedance at 20 Hz when 50 ppm pulses of NO, NO_2 and the 50:50 NO+NO_2 mixture were introduced to the sensor with 5% and 10% O_2 present. The first pulse of NO was introduced at 30 sec, followed by NO_2 at 90 sec, and then a mixture of NO+NO_2 at 150 sec. Data was recorded over 4 cycles at 650°C.

of the electrode) it is clear from the imaginary and phase response that the NO_x response is essentially O_2 independent. This observation suggests that there may be different reaction paths at the electrode for O_2 and NO_x. Finally, for all of the data shown in figure 3 as the signal amplitude increased the absolute value of the real, imaginary, and phase response decreased. The NO_x and O_2 sensitivity were not impacted by the applied signal amplitude.

Figure 4 further illustrates the behavior of the real, imaginary, and phase components as a function of NO and O_2. There was an upward drift in the real impedance response as the repeated measurements following 6 hours of operation resulted in higher impedance values (see figure 4a). This indicates that the resistance of the LCM sensor increased relatively quickly over time. The nature of the electrode reactions is not currently understood. Equally problematic was the poor NO sensitivity as the 10 – 50 ppm NO concentration steps did not result in discrete responses. Alternatively, the imaginary response shown in figure 4b depicts a far more stable behavior along with well-defined responses to NO. The phase response plotted in figure 4c had features similar to the imaginary response, and also demonstrated a stronger signal along with greater stability and reproducibility. Likewise, for both the data sets in figures 4b and 4c the O_2 response was rather slow as substantially longer response times were required before the phase response was relatively stable after a change in oxygen concentration; whereas, the NO concentration steps reflected a relatively rapid response. This again points to different reaction paths at the electrodes for O_2 and NO_x. Interestingly, the O_2 response time improved after about 6 hours of data collection. Overall, these observations suggest that it would be necessary to measure and control the O_2 concentration at the LCM sensor to promote accurate operation.

Figure 4

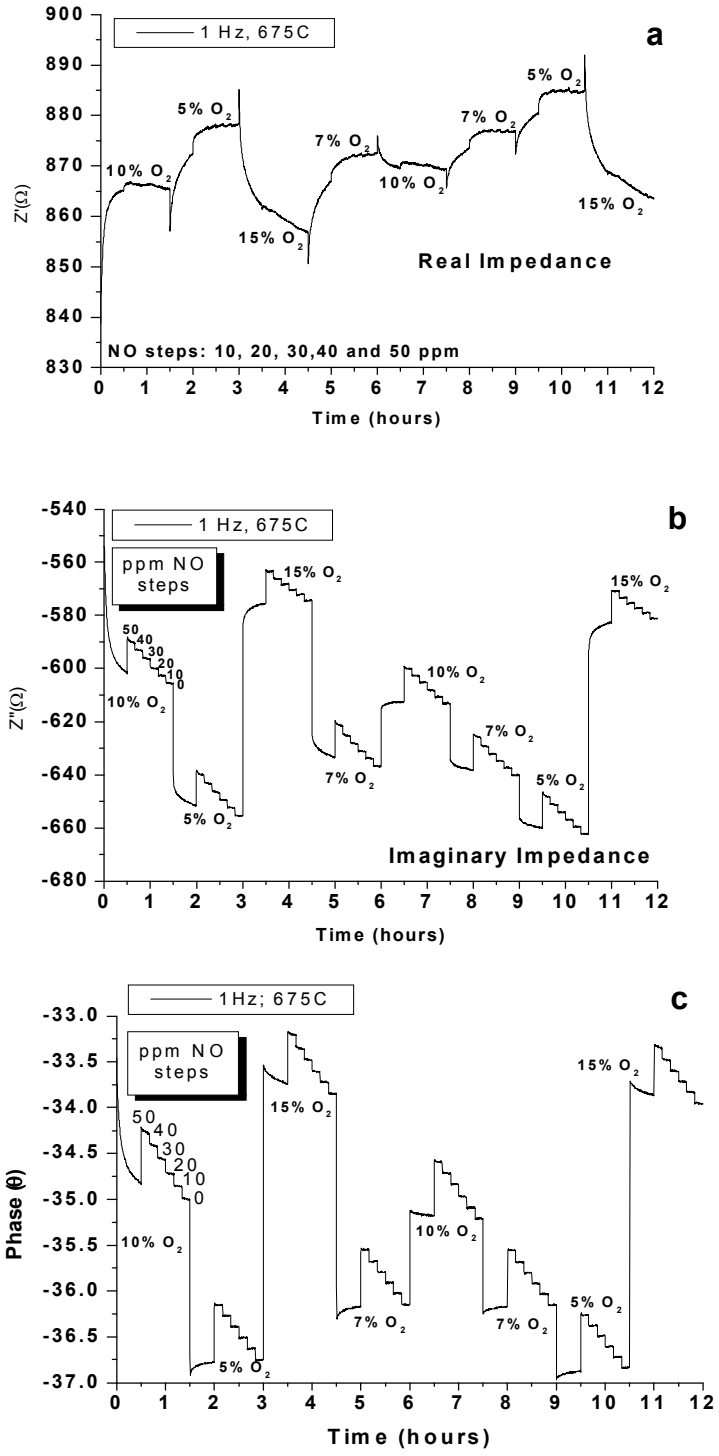

Figure 4. The sensor response is shown for the a) real, b) imaginary, and c) phase components of the impedance as a function of NO and O_2 concentration.

The phase response for NO is compared to those for NO_2 and the 50:50 NO+NO_2 mixture in figures 5a and 5b for constant frequency measurements collected at 1 Hz and 5 Hz. For each frequency the NO response was not as strong or pronounced as the response to the concentration steps for NO_2 and the 50:50 NO+NO_2 mixture. Further comparisons indicate the 1 Hz measurements resulted in a stronger response to NO_x along with greater distinction between the 2 ppm increments in NOx. This demonstrates that small changes in NO_x concentration can be resolved by the phase response. Some caution is warranted as the 50:50 NO+NO_2 gas mixture data overlapped with some of the sensor responses for NO_2. For 28 ppm NO_2 the phase response was nearly identical to that for 20 ppm NO+NO_2. This is problematic as it indicates that 10 ppm NO mixed with 10 ppm NO_2 generates the same response as 28 ppm NO_2. So, for such a sensor an operating strategy would need to be employed, such as converting NO_2 to NO, to avoid erroneous measurements. This could easily be accomplished with a Pt-based catalyst operated at sufficiently high temperature and located upstream of the sensor.

Figure 5

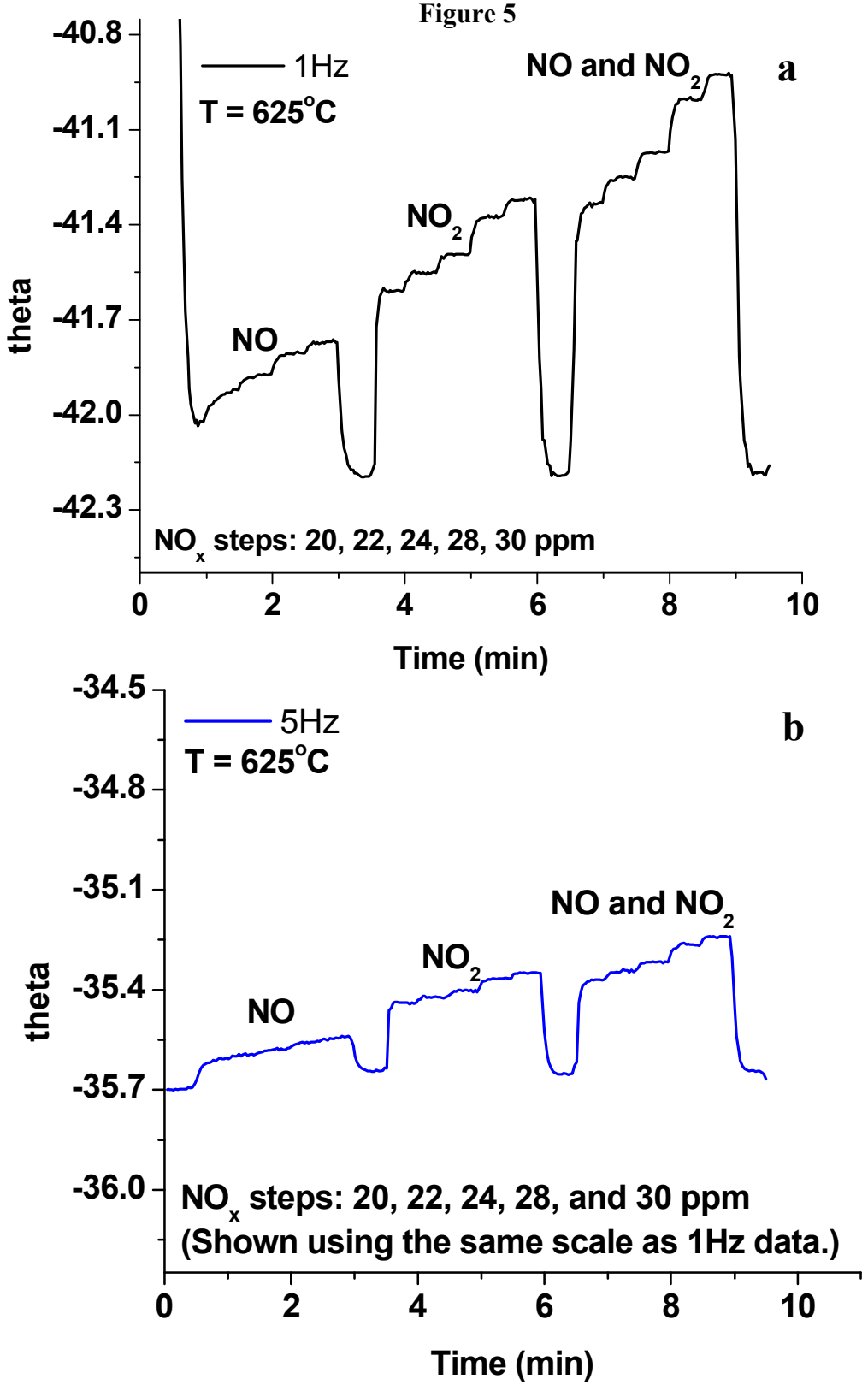

Figure 5. NO_x sensitivity measurements at constant frequencies of a) 1 Hz and b) 5 Hz. The gas concentration steps were 20, 22, 24, 28 and 30ppm for NO, NO_2 and the NO+NO_2 mixture.

Temperature and Frequency Dependence

Typical full spectrum sweeps shown in figure 6 compare the phase response when 50 ppm NO was present to baseline conditions (i.e., N_2 + 5% O_2). There were 3 peaks for each temperature measured and the peak placement was temperature dependent. From approximately 5 – 50 Hz the phase response was relatively unchanged indicating the LCM electrode response was independent of temperature within this frequency range. At 30 kHz another temperature independent point was observed. Unfortunately, where no temperature dependency in the sensor's output was present there was also no response to NO_x. The difference in phase was small between the data sets where 50 ppm NO was present and corresponding baseline data sets. In addition, for frequencies over 2 Hz the phase response was O_2 independent. Figures 6b and 6c further illustrate the O_2 behavior as a function of frequency. The low frequency O_2 dependence observed indicates a practical LCM sensor would require a method for measuring and controlling the O_2 concentration to achieve sufficient accuracy. Additionally, the data indicates the LCM sensor was even more sensitive to temperature in comparison to the O_2 dependence. So, careful management of the operating temperature would also be required. A possible approach would be to monitor the temperature by measuring the phase response at high frequencies, such as $2x10^5$ Hz or greater, as this region is temperature dependent and O_2 independent. From figure 6 it is also apparent that the sensor sensitivity to NO and O_2 is greater for lower temperatures and lower frequencies as the magnitude of the phase response was the largest at those conditions. This is further illustrated in figure 7 where the phase response is plotted as a function of temperature for data collected at 1 Hz, 5 Hz, and peak frequencies. A plot of the peak frequencies is shown in figure 7b as the peak frequency is temperature dependent. The difference between the baseline

response and the NO response decreased with increasing temperature, which has been observed in other studies.[7]

Figure 6

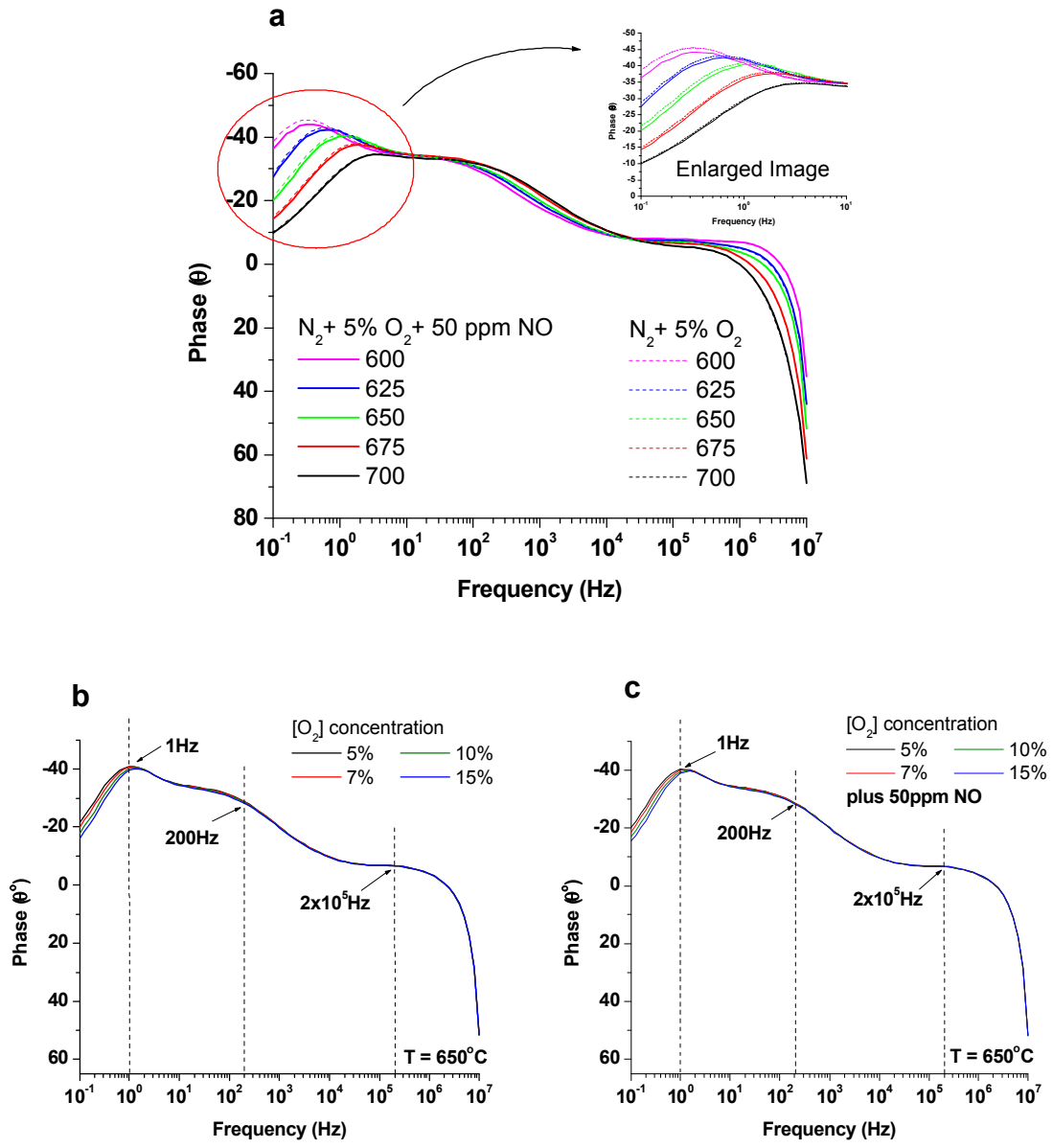

Figure 6. The frequency dependence of the phase response is shown for a) temperatures ranging from 600 – 700°C, and as a function of O_2 concentration b) without any NO present, and c) with 50 ppm NO.

Figure 7

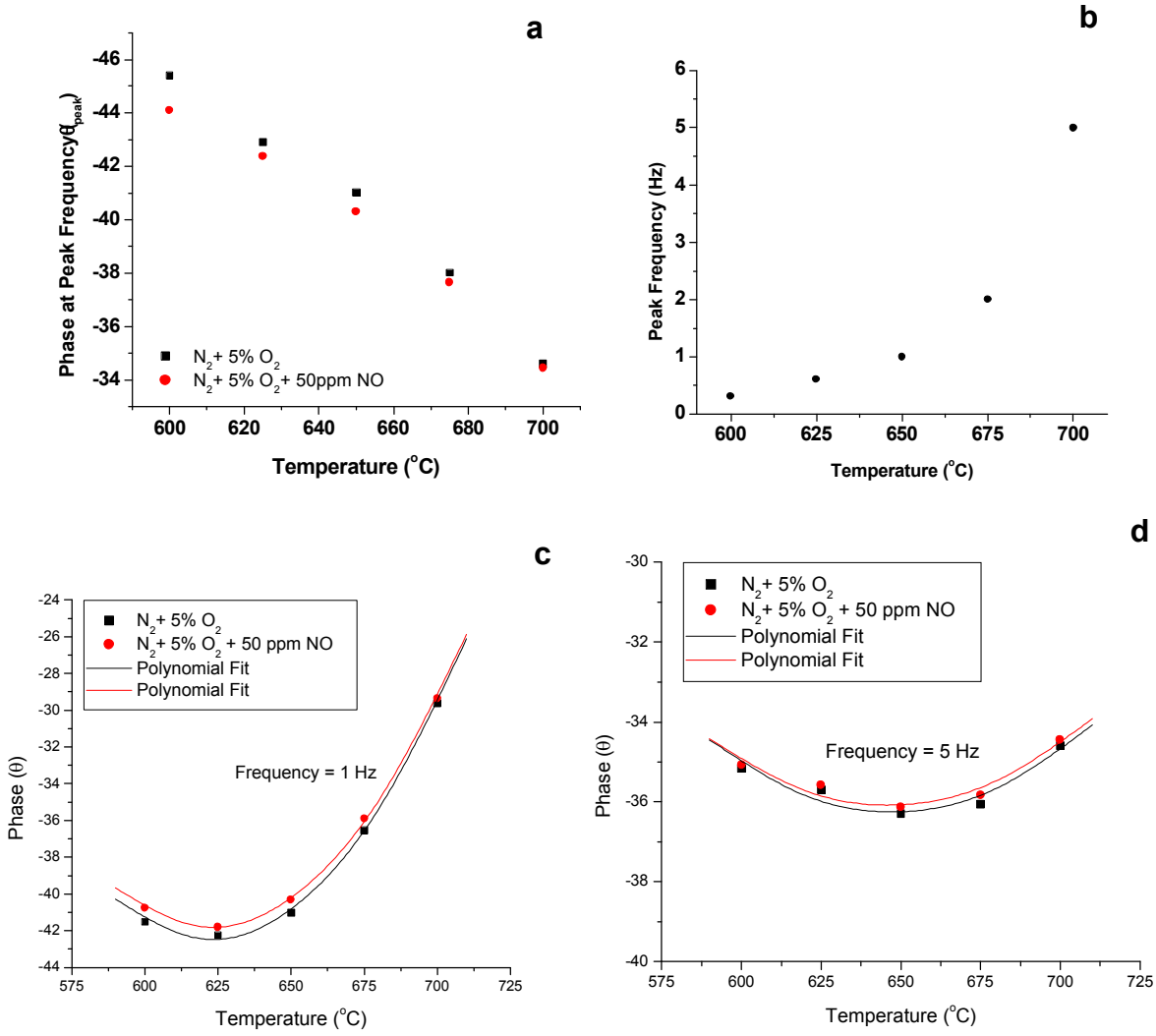

Figure 7. The phase response is shown as a function of temperature for data collected at the a) peak frequencies where the specific peak frequency values are plotted in b). The temperature dependence is also illustrated for constant frequencies of c) 1 Hz, and d) 5 Hz.

Comparisons of the data shown in figures 7a, 7c and 7d indicate the largest response to NO occurs at 600°C (in figure 7a) at the peak frequency that is approximately 0.3 Hz. Unfortunately, operating a sensor at 0.3 Hz is too slow for a practical NO_x sensor. Additionally, at 0.3 Hz the LCM sensor is quite sensitive to temperature. In figures 7c and 7d it is apparent that the phase goes through a minimum value, which is a function of frequency and temperature. The smallest

change in phase as a function of temperature (i.e., $d\theta/dT$) occurs at this minimum. These findings indicate that the optimal operating conditions for measuring the phase response are significantly influenced by the temperature and frequency dependence of the phase response.

If the sensor operating temperature were precisely known, then the sensor could be periodically calibrated to measure the actual NO concentration present. However, it is more likely that the sensor operating temperature will be unknown to within ± 5°C. Table 1 is based on further analysis of figure 7, and shows the change in the phase response ($\Delta\theta$) and resulting NO

Table 1: Change in sensor phase response and corresponding NO measurement when the sensor operating temperature is not precisely known. Data is shown for 1 Hz and 5 Hz for 650°C.

Table 1

	Temperature (°C)	$\Delta\theta$ (degrees) ($\Delta\theta = \theta_{baseline} - \theta_{NO}$)	NO measurement (ppm)
1 Hz	650°C	0.70°	50
	+5°C perturbation (T=655°C)	1.32°	94
	-5°C perturbation (T=645°C)	0.21°	15
5 Hz	650°C	0.17°	50
	+5°C perturbation (T=655°C)	0.24°	71
	-5°C perturbation (T=645°C)	0.21°	62

Table 2: Change in sensor phase response and corresponding NO measurement for the minimum $d\theta/dT$ occurring at 625°C for 1 Hz (see figure 7c).

Table 2

	Temperature (°C)	$\Delta\theta$ (degrees) ($\Delta\theta = \theta_{baseline} - \theta_{NO}$)	NO measurement (ppm)
1 Hz	625°C	0.67°	50
	+5°C perturbation (T=630°C)	0.75°	56
	-5°C perturbation (T=620°C)	0.69°	52

concentration measurement. At 650°C when 50 ppm NO was present the LCM sensor resulted in a phase change of 0.70° and 0.17° for constant frequency measurements at 1 Hz and 5 Hz, respectively. A + 5°C or – 5°C perturbation at 650°C would result in an erroneous NO measurement of 94 ppm or 15 ppm, respectively at 1 Hz. At 5 Hz and 650°C the temperature dependence is less. As shown in Table 1 for these conditions a 50 ppm NO response would be interpreted as 71 ppm or 62 ppm NO if the temperature fluctuated by + 5°C or – 5°C, respectively; thereby, indicating a sensor accuracy of 60 ± 10 ppm. Operating the sensor at 5 Hz and 650°C coincides with the minimum $d\theta/dT$ (see figure 7d). For 1 Hz operation the minimum $d\theta/dT$ occurs at 625°C, as shown in figure 7c. Table 2 shows $\Delta\theta$ and the corresponding NO concentration for sensor operation at 625°C along with perturbations of ± 5°C. Under these operating conditions the LCM sensor accuracy is much improved as a 50 ppm NO response could be read by the sensor as 53 ± 3 ppm. Prior work by the authors where a DC approach was used to measure NO_x sensitivity determined that a ± 5°C temperature fluctuation resulted in a ± 5 ppm error in the NO response.[7] The work in the present study demonstrates that using an AC phase response approach may offer greater accuracy, in addition to better stability. This accuracy strongly depends upon the operating temperature, frequency and minimum $d\theta/dT$. In addition, response time and other noise factors, such as oxygen dependency, need to be taken into account as well.

Temperature dependent impedance measurements are plotted in figure 8a. Closer examination of the data indicated that 3 impedance arcs were present (see figure 8b). The high frequency arc (HFA) had a peak around 200 Hz and the subsequent low frequency arcs, referred to as LFA1 and LFA2, generated peaks at about 63 Hz and 0.4 Hz, respectively. The lowest

Figure 8

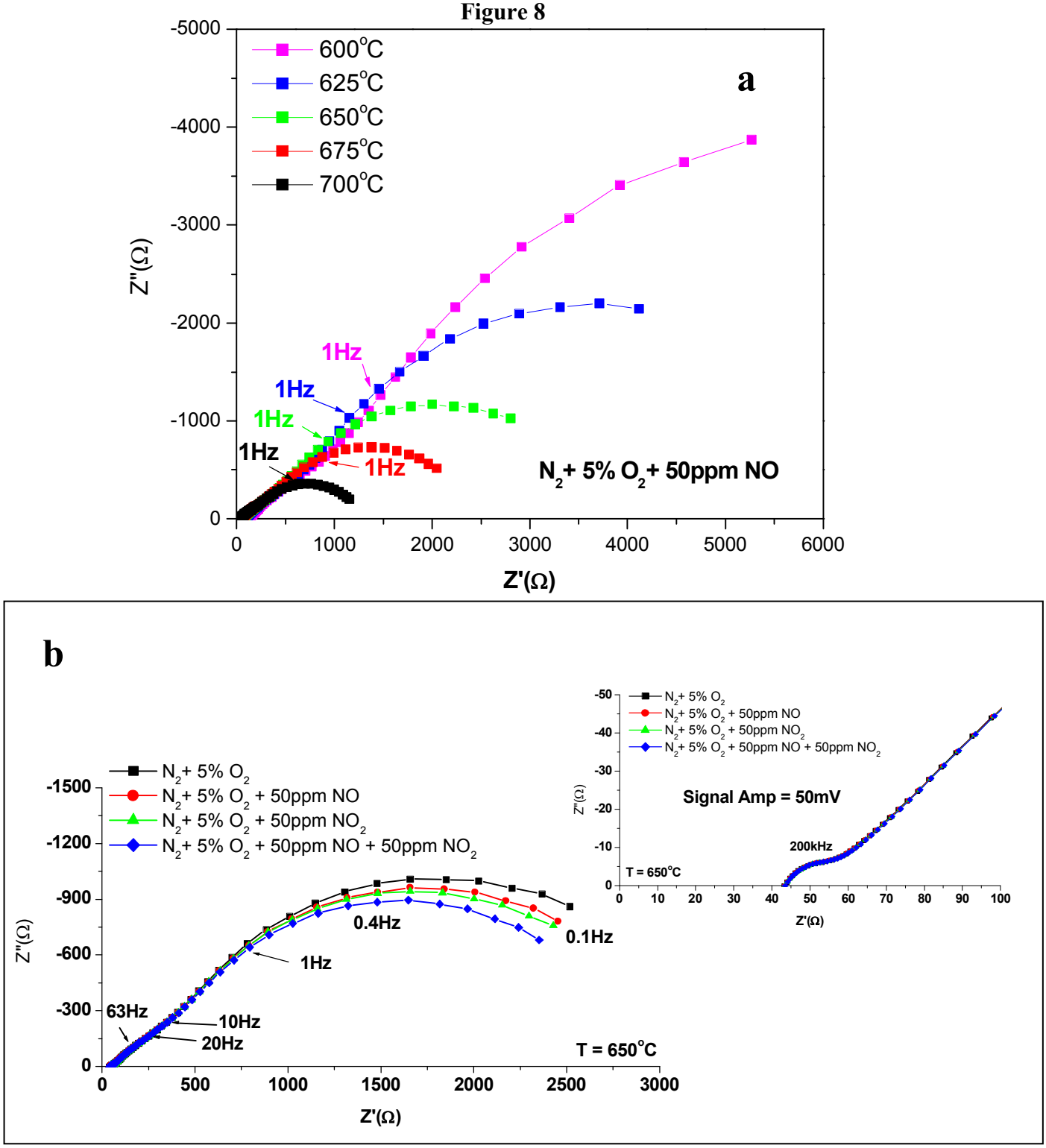

Figure 8. a) The temperature dependence of the real and imaginary impedance is shown for 600 - 700°C. b) The low frequency arcs and the enlarged view of the small high frequency arc are illustrated for various concentrations of NO_x.

impedance arc was usually an incomplete arc suggesting charge transfer was a rate limiting step. This was most evident at lower operating temperatures as shown in figure 8a. The activation energy calculated for the HFA, LFA1 and LFA2 were 1.37±0.02 eV, 1.23±0.11 eV and 1.73±0.06 eV, respectively. These are relatively high values, particularly the HFA which most likely corresponds to reactions occurring at the YSZ electrolyte. The high frequency associated with this arc and the fact that the arc is independent of gas composition (see figure 8b) is characteristic of the bulk YSZ electrolyte impedance response. However, the activation energy for YSZ is typically 0.96 eV for temperatures over 550°C.[9] SEM analysis of the sensor at the conclusion of this study indicated dark regions within the YSZ electrolyte substrate located beneath the various LCM/YSZ interfaces (see figure 9). Interestingly, the dark regions did not span the entire area of the electrode but instead were confined to an area under the Ag-Pd overlay. Though the electrode/electrolyte reactions causing such a microstructural change are not understood, such a result quite likely was the reason for the high activation energies. Most experiments were carried out using a signal amplitude of 50 mV. The maximum amplitude applied was 100 mV. Although these voltages are very low some blackening of the zirconia may have occurred. However, the mechanism is unclear as a pumping current was present. Blackening of ZrO_2 is generally understood to take place when a voltage is present without a current. These SEM observations indicate the LCM sensor was changing while measurements were being made. Since baseline measurements that were repeated at the end of each testing day verified reproducible data, it appears that the changes occurring at the LCM sensor took place over several days.

Figure 9

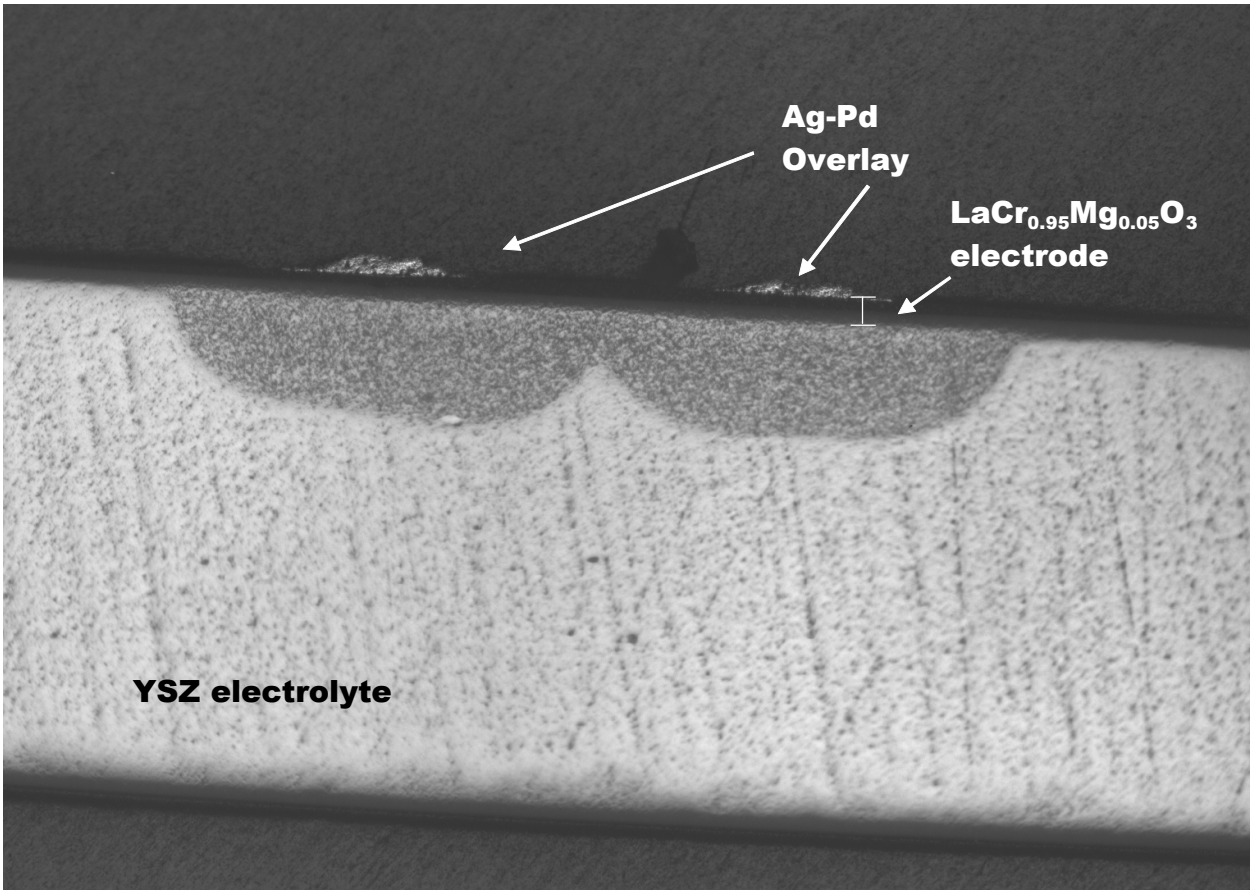

Figure 9. SEM image of a cross section of the LCM/YSZ sensor showing dark regions, (possibly blackened zirconia) that formed within the YSZ electrolyte.

Stability and Accuracy of the Phase Response

A comparison between measurements collected over time, shown in figure 10, indicate the tolerance of the real, imaginary and phase components for instability in the electrode response. The real and imaginary impedance described in figure 10a indicated LFA2 significantly increased over 11 days of testing. During that time various experiments, including those described in this paper were performed. The increase in the impedance was nearly the same for the baseline measurements and those where 50 ppm NO was added. The phase response in figure 10b over the same time period reflects a smaller change between the two sets of measurements. Apparently, the phase response was more tolerant to changes in the electrode response in comparison to the real and imaginary components of the impedance response. In addition, the phase response indicated a change occurred at higher frequencies, which was not readily observed in the impedance measurements. Figure 10c shows how much the response for the real, imaginary, and phase components changed over 11 days of sensor operation by showing the percentage increase in the response for each component over the frequency range measured. The sensor response was most sensitive to changes in the sensor response at frequencies below 1 Hz. The phase response appears to be far more tolerant to instability in the sensor response as the percent change between the initial and final measurements was about 2% or less for frequencies above 1 Hz. The data in figure 5a is useful for interpreting how much a 2% change in the sensor response effects sensor accuracy. According to the data here a 2% change in the phase response corresponds to roughly 0.8°. It is apparent that the phase response increased by just about 0.05° when the NO_x concentration increased by 2 ppm. Hence, considering the drift in the phase response the best accuracy for the LCM sensing electrode is 32 ppm for NO. Although this value exceeds the accuracy requirement of < 2 ppm NO_x, the phase response of the sensor

demonstrated far better accuracy in comparison to the prior DC measurement approach previously studied by the authors.[7]

Figure 10

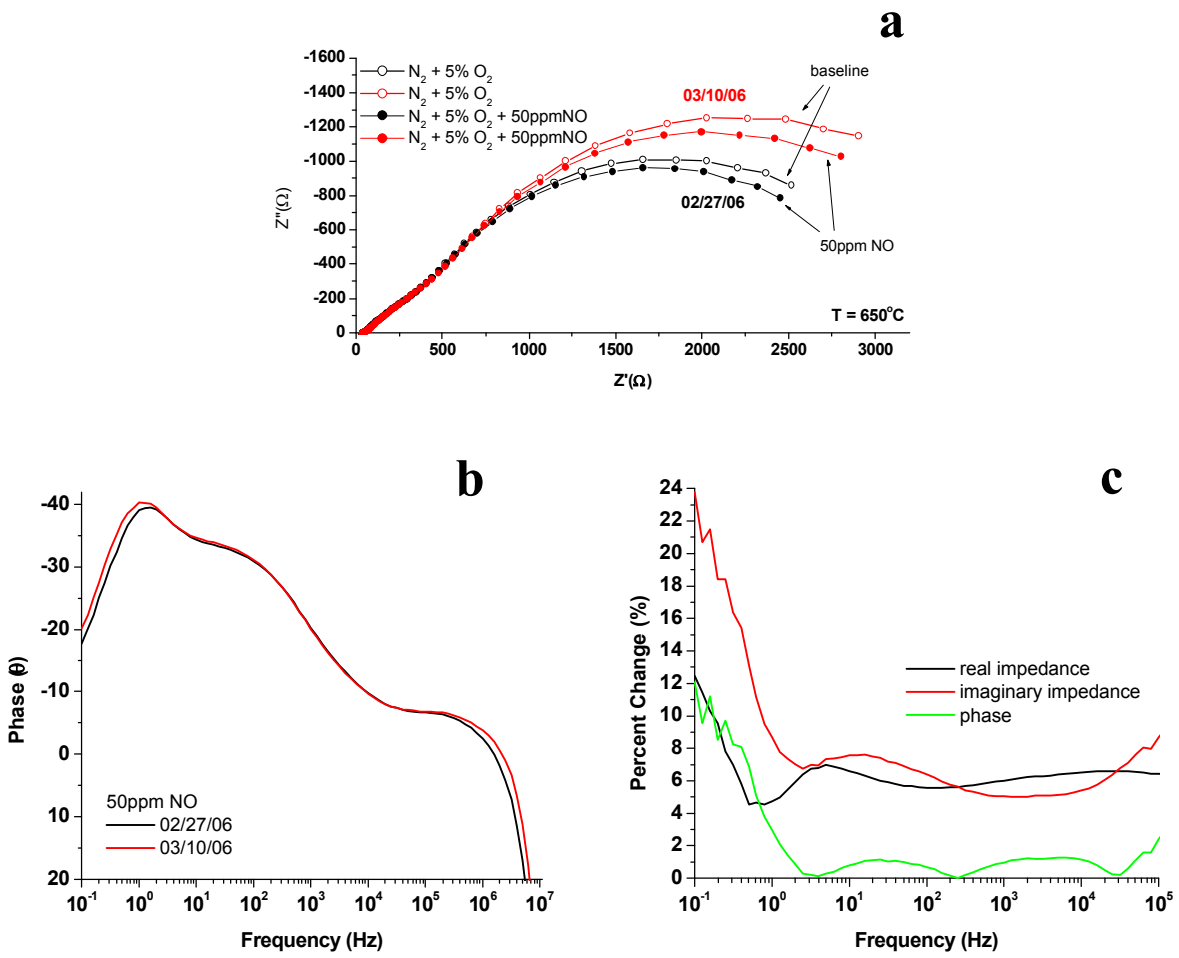

Figure 10. a) A comparison of the sensor performance before and after 11 days of testing indicated significant changes in the impedance response. b) The corresponding phase response shows a slight difference between the data sets at very low and very high frequencies with negligible difference over a large frequency range. c) The percent change between the initial data and data collected 11 days later is shown for the real and imaginary impedances and the phase response.

Conclusions

The phase response of the LCM electrode demonstrated sensitivity to NO_x, as well as O_2 and temperature. Oxygen sensitivity was reflected in the baseline response of the sensor, but appeared to have a negligible effect on the magnitude of the NO_x response. The O_2 and temperature sensitivity indicated that careful monitoring of these variables would be required to promote accurate sensor operation. The real impedance response was sensitive to O_2 but not to NO_x; whereas, the imaginary impedance response was sensitive to both O_2 and NO_x. The behavior of the real and imaginary impedance responses indicated that the NO_x changed the capacitance of the LCM electrode. Measurements with the 50:50 NO+NO_2 mixture demonstrated overlapping phase responses with NO_2, which suggested that conversion of NO_2 to NO could reduce the potential for erroneous measurements. Overall, the phase response was far more stable in comparison to the real and imaginary impedance responses.

The temperature dependence for operation at 1 Hz and 5 Hz indicated the accuracy of the AC phase response approach strongly depends upon the operating temperature, frequency and $d\theta/dT$. Data analysis for operation at 1 Hz and 625°C where the LCM sensor accuracy for NO was 53 ± 3 ppm validates the fact that the AC phase response approach is quite promising for achieving highly accurate NO concentration measurements. However, the large accuracy error associated with drift in the LCM electrode response over days of operation must be overcome to achieve a viable NO_x sensor. The large temperature dependence and material instability is a major concern for this sensor. Thus, further study is necessary to identify more suitable electrode/electrolyte systems. Future work will also involve measurements made in humidified atmospheres as the presence of water vapor is known to affect the NO_x sensor response.[10]

Acknowledgements

The authors would like to thank Leta Woo, L. Peter Martin and Robert S. Glass of Lawrence Livermore National Laboratory for participating in useful technical discussions regarding the NOx sensor phase response. Work performed for DOE by UC, LLNL under Contract W-7405-Eng-48.

References

1. Y-W. Kim and M. Van Nieuwstadt, "Threshold Monitoring in Urea SCR Systems", SAE Technical Paper #2006-01-3548.
2. S. Akbar, P. Dutta and C. Lee, "High-Temperature Ceramic Gas Sensors: A Review", Int. J. Appl. Ceram. Technol., 3 [4] 302-311 (2006).
3. S. Zhuiykov and N. Miura, "Development of zirconia-based potentiometric NO_x sensors for automotive and energy industries in the early 21^{st} century: What are the prospects for sensors?", Sensors and Actuators B, in press (2006).
4. T. Ono, M. Hasei, A. Kunimoto and N. Miura, "Improving of sensing performance of zirconia-based total NO_x sensor by attachment of oxidation catalyst electrode", Solid State Ionics **175** (2004) 503-506.
5. N.F. Szabo and P.K. Dutta, "Correlation of sensing behavior of mixed potential sensors with chemical and electrochemical properties of electrodes", Solid State Ionics **171** (2004) 183-190.
6. J. Sfeir, "$LaCrO_3$-based anodes: stability considerations", Journal of Power Sources **118** (2003) 276-285.
7. E. Perry Murray, R.F. Novak, J.H. Visser, D.J. Kubinski and R.E. Soltis, "Characteristics of the NO_x Sensing Behavior of $LaCr_{0.95}Mg_{0.05}O_3$ Electrodes", in preparation.
8. S. Zhuiykov, T. Ono, N. Yamazoe and N. Miura, "High-temperature NO_x sensors using zirconia solid electrolyte and zinc-family oxide sensing electrode", Solid State Ionics **152** (2002) 801-807.
9. C.-C.T. Yang, W-C. J. Wei and A. Roosen, "Electrical Conductivity and Microstructures of $La_{0.65}Sr_{0.3}MnO_3$ – 8-mol% Yttria-stabilized Zirconia", Materials Chemistry and Physics **81** (2003) 134-142.
10. J. Yoo, H. Yoon, and E.D. Wachsman, "Sensing Properties of MO_x/YSZ/Pt (MO_x = Cr_2O_3, SnO_2, CeO_2) Potentiometric Sensor for NO_2 Detection" Journal of the Electrochemical Society, **153**, H217 – H221 (2006).